Obtaining Low-Frequency Spectra of Acetone Dissolved in Cyclohexane by Terahertz Time-Domain Spectroscopy

Partha Dutta[†,‡] **and Keisuke Tominaga***[,†,‡]

Core Research for Evolutional Science and Technology, Japan Science and Technology Agency, Kobe University, Nada, Kobe 657-8501, Japan, and Molecular Photoscience Research Center, Kobe University, Nada, Kobe 657-8501, Japan

Received: January 16, 2009; Revised Manuscript Received: May 29, 2009

We have performed measurements of the low-frequency spectra of the refractive index and the extinction coefficient of solutions of acetone in cyclohexane at concentrations ranging between 27 and 135 mM by using terahertz time-domain spectroscopy (THz-TDS) at room temperature. We have verified Beer's law for the concentration range of our experiment, which establishes the fact that the solute−solvent interaction has a significant contribution to the observed spectra, whereas the interaction between the solute molecules is negligible in the present experimental conditions. Combining the data reported by Vij and Hufnagel (*J. Phys. Chem.*, **1991**, *95*, 6142) with the results of the present experiments, an analytical model for the time correlation function for the total dipole moment of the system was examined in order to reproduce the low-frequency spectra. The molecular origins of the components in the TCF are discussed in light of the results of our simulation.

1. Introduction

The molecular dynamics of liquids has been a fundamental research topic in chemistry since the solute−solvent interaction and dynamics play a key role in chemical reactions.[1,2] Dielectric relaxation in the megahertz and gigahertz regions are often dominated by the orientational motion of the molecules, which can be described by several theoretical models, including the Debye theory.[3,4] The Debye relaxation time characterizes the time scale of the orientational motion, which depends on the bulk viscosity of the system, which is in turn described by the Stokes−Einstein−Debye (SED) equation.

The dynamics of the interaction in the solution are often characterized by time scales ranging between subpicoseconds to tens of picoseconds, which correspond to the terahertz and gigahertz spectral ranges in the frequency domain, respectively. The high-frequency response might be due to intermolecular vibration, librational motion, structural fluctuation of the hydrogen bonding network, as well as intramolecular large-amplitude motion. The high-frequency dielectric response is especially important for understanding the ultrafast component in the solvation dynamics.[5,6] It has often been observed that the initial response of the solvation dynamics takes place in less than 100 fs, which is due to the inertial motion of the solvent molecules.[6] In order to understand this ultrafast response of the solvent on a quantitative level, it is necessary to obtain accurate data regarding the dielectric response in the high-frequency region.

The response of liquids in the terahertz region has often been studied by utilizing optical Kerr effect (OKE) spectroscopy, in which a femtosecond pump pulse creates transient anisotropy in the refractive index, whose relaxation is probed by a second pulse.[7−11] The dynamical response of molecules in liquids and liquid mixtures has been widely studied with this method. However, the technique is not suitable for studying the interaction between solute and solvent molecules in solutions since in this case the contribution of the solvent must be subtracted from the spectrum of the solution, and the OKE measurement, which is intrinsically a scattering method, requires an internal reference for normalizing the spectra.

On the other hand, transmission spectroscopy is suitable for studying the properties of the solute molecules in solutions since the contribution of the solvent can be subtracted from the spectrum of the solution. Traditionally, a combination of microwave and far-infrared (FIR) spectroscopy (FT-FIR) has been used for the terahertz or the FIR region in order to obtain the low-frequency spectrum directly, as there has been no conventional source which covered both regions.[12,13] Also, line tunable FIR lasers at several discrete wavelengths in the low-frequency region have been used to detect the low-frequency spectrum.[14,15] However, due to the limited sensitivity of the apparatus, the results of the experimental detection of the spectrum with this method might include rather large error bars, which could eventually produce ambiguity in the analysis.

Recently, terahertz time-domain spectroscopy (THz-TDS) has received considerable attention in studies of low-frequency spectra in condensed phases.[16,17] THz-TDS measures the time evolution of the electric field of the radiation propagating through a sample, providing the phase and amplitude changes of the radiation. Therefore, the refractive index and the absorption coefficient of the sample are obtained in the form of complex dielectric spectra. Development has recently taken place in the coherent generation and detection of light pulses in the terahertz range. Depending on the technology used in the emitter and the detector, the frequency region covered by this technique is 0.1−10 THz.

The technique has been applied to studies on liquid and liquid mixtures, and the results were in terms of some analytical model to obtain insight of the microscopic dynamics of the system.[18−20] In this work, we have performed a series of such THz-TDS

* Corresponding author, tominaga@kobe-u.ac.jp, Molecular Photoscience Research Center, Kobe University.
† Core Research for Evolutional Science and Technology, Japan Science and Technology Agency.
‡ Molecular Photoscience Research Center.

10.1021/jp900488c CCC: $40.75
Published on Web 07/01/2009

studies on different solutions. The chemical system we use is a solution of acetone in cyclohexane. So far, we have studied the low-frequency spectra of solutions of polar aromatic solute molecules in nonpolar solvents.[21−23] By subtracting the solvent part from the spectrum of diluted solution, we obtained the contribution of the solute from the solute−solvent interaction, which was analyzed by utilizing a theoretical function for the time correlation function (TCF) of the total dipole moment of the system. We investigated the dependence of the spectra on the solute concentration, which is essential for the study of the solute−solvent interaction. If Beer's law is not followed, the solute−solute interaction has to be included in the analysis and discussion. The acetone/cyclohexane system has been previously studied by using a combination of line tunable FIR lasers at several discrete wavelengths and FT-FIR spectroscopy in the low-frequency range.[15] By combining the previous data and the data obtained in the present work, we analyzed the dynamics and the interactions in this system by using a model analytic TCF of the solute dipole moment. We also discussed the general necessity of introducing an additional high-frequency component besides the orientational diffusive relaxation in order to simulate the low-frequency spectra.

In recent years, several groups have studied the concentration dependence of aqueous solutions on the viewpoint of different physical parameters related with the hydrated water molecules using terahertz spectroscopy.[24−27] Tanaka and co-workers studied concentration dependence of the complex dielectric constant to show that the hydration number decreases with increasing concentration of sucrose and trehalose.[24,25] Havenith and co-workers reported a nonmonotonic change in the terahertz absorption coefficient with the change in the concentration of lactose solution.[26] They also reported that for the carbohydrates, the solute-induced change in the terahertz absorption depends on the product of molar concentration of the solute and the number of hydrogen bonds between the carbohydrate and water molecules and found that monosaccharides have a smaller influence on the surrounding water molecules than disaccharides.[27]

2. Experimental Section

We used two different THz-TDS methods, one of which is based on the electro-optic sampling (EO) method and the other of which involves the use of a photoconductive (PC) antenna system. The first method has been described in detail elsewhere.[31,32] As a brief overview, in this method, femtosecond pulses from a mode-locked titanium sapphire laser are used for generating and detecting pulsed terahertz radiation. Most of the pulses are focused on the (100)-surface of an InAs wafer. The wafer is placed in a magnetic field with a flux density of 1.6 T in order to enhance the intensity of the radiation. The rest of the pulses are used for detecting the electric field of pulsed terahertz radiation with the EO sampling method by using a ZnTe crystal. This system covers the frequency range between 15 and 85 cm^{-1}. The power spectrum of the terahertz radiation has a small intensity above 85 cm^{-1}, so that the spectra of refractive index and absorption coefficient are noisy in that region. The other method uses a PC system for generating and detecting terahertz radiation (AISPEC Inc.), which is produced by femtosecond pulses from a mode-locked titanium sapphire laser. This apparatus covers the frequency range between 2 and 50 cm^{-1}. The measurements were performed at room temperature (293 ± 1 K), and the sample solutions were placed in cells with Teflon windows with an optical path length of 15 mm. Acetone and cyclohexane samples (Wako Pure Chemicals) were used without further purification. The concentration range of the solution was between 27 and 135 mM.

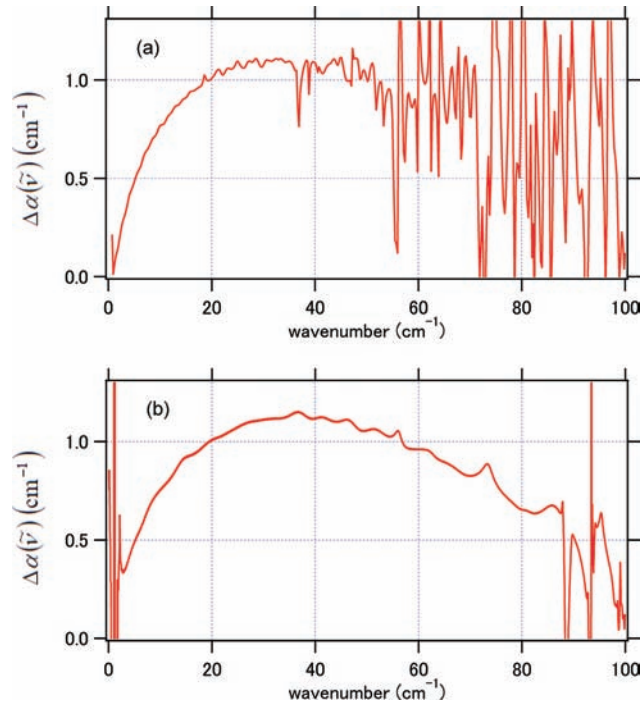

Figure 1. Plot of $\Delta\alpha(\tilde{\nu})$ for the 135 mM solution of acetone in cyclohexane and the pure solvent cyclohexane as a function of the wavenumber obtained by using (a) a PC antenna THz-TDS setup and (b) EO sampling THz-TDS setup.

We combined the spectra obtained with the two methods. Figure 1 shows the spectra obtained with the two methods. In the combined spectrum (Figure 2a), the lower wavenumber region (2−30 cm^{-1}) of the spectrum was measured by using the PC THz-TDS setup, and the higher wavenumber region (30 to 85 cm^{-1}) was obtained by using the EO-sampling THz-TDS setup. The combined spectra are free from any kind of scaling in either of the methods. The experimental data for the range between 2 and 70 cm^{-1} have been used for analysis.

In the above measurements, we obtained the difference spectra of the refractive index $\Delta n(\tilde{\nu})$ and the absorption coefficient $\Delta\alpha(\tilde{\nu})$ between the sample and reference cells. The expressions of $\Delta n(\tilde{\nu})$ and $\Delta\alpha(\tilde{\nu})$ have been described elsewhere.[31,32] Thus, in order to obtain the spectra of the solutions, we first performed measurements with the sample cell and the reference cell containing the solutions and the pure solvents, respectively. After this, we obtained the spectra for the sample cells filled with the solvents and the empty reference cell. By assuming that the refractive index and the absorption coefficient of air are unity and zero, respectively, we obtained the respective spectra of the refractive index and the absorption coefficient of the solvents in the frequency range examined in these experiments. We calculated the sum of the difference spectra between the solutions and the solvents and the difference spectra between the solvents and air in order to obtain the solution spectra $n_{soln}(\tilde{\nu})$ and $\alpha_{soln}(\tilde{\nu})$.

3. Results and Discussion

3.1. Spectral Measurements and Concentration Dependence. We measured the difference spectra of the refractive index ($\Delta n(\tilde{\nu})$) and the absorption coefficient ($\Delta\alpha(\tilde{\nu})$) between the solution of acetone in cyclohexane and the solvent cyclohexane (Figure 2). From Figure 2, it is clear that $\Delta n(\tilde{\nu})$ decreases

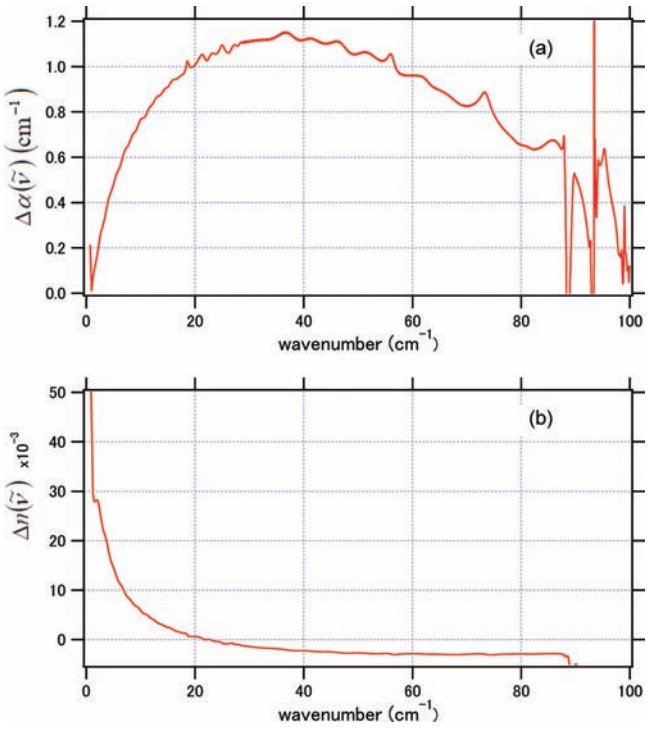

Figure 2. Plots of (a) $\Delta\alpha(\tilde{\nu})$ and (b) $\Delta n(\tilde{\nu})$ between the 135 mM solution of acetone in cyclohexane and the pure solvent cyclohexane as a function of the wavenumber.

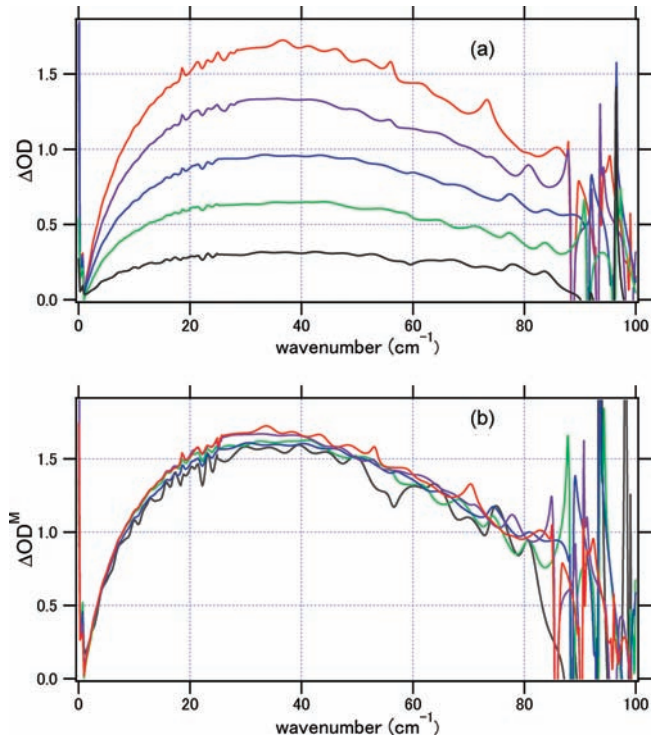

Figure 3. Plots of (a) the difference in the spectral intensity of absorption (ΔOD) between the solution of acetone in cyclohexane and the solvent cyclohexane as a function of the wavenumber for the following concentrations of acetone: 27 mM (black), 54 mM (green), 81 mM (blue), 108 mM (violet), and 135 mM (red). (b) Plots of ΔOD^M, the difference in the spectral intensity of absorption between the solution of acetone in cyclohexane and the solvent cyclohexane as a function of the wavenumber as normalized by the concentration: 27 mM (black), 54 mM (green), 81 mM (blue), 108 mM (violet), and 135 mM (red).

as the wavenumber increases in the low-frequency range, while it is almost constant at higher frequencies. This behavior is quite similar to that of other polar solutes in nonpolar solvents.[21−23]

We adjusted the concentration of acetone in cyclohexane in the range between 27 and 135 mM. Figure 3a shows the changes in the difference spectra of absorption (ΔOD) between the acetone/cyclohexane solution and the solvent cyclohexane. In Figure 3b, the vertical axis represents the optical density, which is divided by the concentration in order to obtain the molar absorptivity (ΔOD^M). This figure shows that the magnitude is within 10% in comparison to the values of the lower concentration and the spectral shapes of ΔOD^M for all the concentration levels are almost identical. Thus, it indicates the validity of Beer's law in this experimental concentration range, and it can be reasonably assumed that the interaction between the solutes is almost negligible, as well as that only the solute−solvent interaction plays a role in interpreting the terahertz spectra.

In this context, it should be discussed that Flanders et al. also performed concentration variation of chloroform in the mixtures of chloroform and carbon tetrachloride using the THZ-TDS technique.[18] As they used a higher concentration of chloroform in the solution, they found that their spectra did not verify Beer's law; rather, the interaction term between different solutes which is different than the interaction between different solvent, plays a major role to discuss the origin of the THz-TDS spectra.

3.2. Comparison with Previous Studies. Vij and Hufnagel reported dielectric loss in the frequency range between 2 and 150 GHz as well as the power absorption coefficient in the range between 300 GHz and 6 THz for dilute solutions of aliphatic ketones (including acetone) in cyclohexane at 20 °C.[15] Their measurements were performed at selected spot frequencies, which are denoted with red points in Figure 4. The present data are superimposed on the previous data in log scale, as shown in Figure 4a. Here, we compare the difference spectra of the imaginary part of the dielectric permittivity ($\Delta\varepsilon''(\tilde{\nu})$) between the acetone/cyclohexane solution and the pure solvent cyclohexane as observed in our study with those reported by Vij and Hufnagel. For all solutions, we found that the maximum of $\Delta\varepsilon''(\tilde{\nu})$ is at around 3.6 cm^{-1}, which coincides with the result of the previous work mentioned above. We plotted the data for $\Delta\varepsilon''(\tilde{\nu})/f_2$ as obtained from both studies as a function of the wavenumber, where f_2 is the mole fraction of the solute.

Figure 4a shows the difference in the experimental data between the present and previous studies. The essential point of the difference becomes clearer if we simulate the data by the theoretical model. We performed a simulation of the combined spectrum in Figure 4b (blue) in accordance with the model function for $\Delta\varepsilon''(\tilde{\nu})/f_2$ given by Vij and Hufnagel. It was assumed that there are at least three different dynamical processes.

$$\frac{\Delta\varepsilon''(\tilde{\nu})}{f_2} = (a_s - a_\infty)(2\Pi c(\tilde{\nu}))\left\{\frac{a_1\tau_{D_1}}{1 + (2\Pi c(\tilde{\nu})\tau_{D_1})^2} + \sum_{i=2}^{3}\frac{a_i\tau_{D_i}}{(1 - 4\Pi^2 c(\tilde{\nu})^2\tau_{D_i}\tau_{J_i})^2 + (2\Pi c(\tilde{\nu})\tau_{D_i})^2}\right\} \quad (1)$$

where $a_s = \varepsilon_{soln}(0) - \varepsilon_{solvent}(0)$ and $\varepsilon_{soln}(0)$ and $\varepsilon_{solvent}(0)$ are the static dielectric permittivity of the solution and the solvent, respectively, and a_∞ is that at infinite frequency. Furthermore, τ_{D_i} is the relaxation time, and τ_{J_i} is the angular velocity correlation time which corresponds to the mean time between

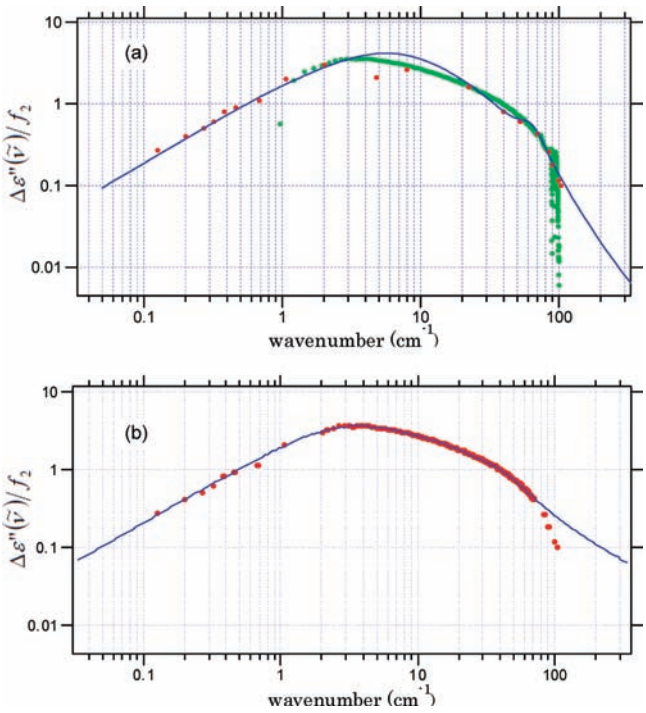

Figure 4. Plots of $\Delta\varepsilon''(\tilde{\nu})/f_2$ for the 135 mM solution of acetone in cyclohexane and the solvent cyclohexane as a function of the wavenumber: (a) Data from ref 15 (red), data from the present THz-TDS experiment (green), and the simulated curve reported in ref 15 (blue). (b) THz-TDS data in the frequency region of 2−70 cm^{-1} are combined with the data reported in ref 15 in the frequency region below 2 cm^{-1} and in the interval of 70−103.6 cm^{-1} (red) and the simulated curve (blue) of the combined data in accordance to eq 1.

TABLE 1: Parameters Obtained from Equation 1 for a System of Acetone Dissolved in Cyclohexane

	a_1	τ_{D_1} (ps)	a_2	τ_{D_2} (ps)	τ_{J_2} (ps)	a_3	τ_{D_3} (ps)	τ_{J_3} (ps)	μ(D)
this work	0.820	1.620	0.149	0.490	0.120	0.031	0.130	0.120	2.73
ref 15	0.089	3.83	0.893	1.0	0.10	0.018	0.042	0.167	2.79

instantaneous collisions which change both the magnitude and the direction of the angular momentum of the molecules. The respective weight factors of the amplitude or the relaxation strengths for the three discrete processes are denoted as a_i, where $i = 1-3$.

The values of the parameters obtained by Vij and Hufnagel are listed in Table 1, and the result for the curve is also shown in Figure 4a. The first term in eq 1 is the essential relaxation process, where the amplitude of this process a_1 is relatively small. The second term ($i = 2$) in eq 1 is also relaxational in character since $\tau_{D_2}/\tau_{J_2} \gg 1$. However, this second component includes an inertial motion characterized by τ_{J_2}. This component has the largest amplitude among the three terms in eq 1. The third process is resonant or librational in character since the value of τ_{D_3}/τ_{J_3} is of the order of unity or less.

We also performed a spectral simulation of the data constructed from present and previous studies. For the frequency region between 2 and 70 cm^{-1}, we used our data, and above and below this region, the data points reported in the above-mentioned previous work were used. The results of the spectral fitting are shown in Figure 4b and Table 1. The quality of the fit is reasonably good except for the high frequency region above 70 cm^{-1}. The major difference between the present and previous spectral fitting is that the first term (1.620 ps) obtained by us corresponds to an average of the first and second terms (3.83 and 1.00 ps) in the previous work, and we emphasize that the two more terms are necessary to reproduce the experimental data properly, while the previous work showed that additional one term was needed, although both the studies simulate in the same spectral region. Moreover, the previous work mentioned that the additional term was highly underdamped; $\tau_{D_3}/\tau_{J_3} \sim 0.25$, which means that this term has an oscillatory feature. We show that the additional two terms are not significantly underdampled; $\tau_{D_2}/\tau_{J_2} \sim 4.1$ and $\tau_{D_3}/\tau_{J_3} \sim 1.1$. The present work shows that the highly accurate measurement in the terahertz region is needed to obtain an adequate picture of the solute−solvent interaction and dynamics.

In the next subsection, we present the obtained spectral simulation by assuming a functional form for the TCF of the total dipole moment of the system. As shown in the previous paragraph, the quality of the spectral simulation is not perfect, although we are aiming to obtain a better fitting. The essential part of the functional form which we eventually obtain is qualitatively similar to that of eq 1, where there are three terms in the TCF, two of which are components in a biexponential function with an inertial component. The time constants of the biexponential decay of these terms are in the picosecond and subpicosecond time ranges. The last term is a Gaussian component with a subpicosecond time constant. In order to justify the simulation, we start with a simple function for the TCF and introduce additional terms into the analytical expression in order to improve the simulation.

3.3. Spectral Analysis. In our previous studies, we demonstrated a method of the spectral analysis in order to reproduce the experimental data accurately.[22,23] In this work, we aim at analyzing the low frequency spectrum in a similar way to investigate the generality of our analytical model. The theoretical background of the analysis has been already discussed in detail.[22,23] Briefly, as the product of the two spectra $\alpha(\tilde{\nu})n(\tilde{\nu})$ is directly related to the Fourier spectrum of the TCF of the total dipole moment of the system ($\mathbf{M}(t)$),[33] the dynamics of the molecules can be discussed from a quantitative point of view by calculating the product $\alpha(\tilde{\nu})n(\tilde{\nu})$ of the spectra of the refractive index and the absorption coefficient, which can be expressed as

$$\alpha(\tilde{\nu})n(\tilde{\nu}) \propto \mathrm{Re}[\tilde{\nu}\{1 - \exp(-hc\tilde{\nu}/kT)\}\int_{-\infty}^{\infty} \mathrm{d}t \times \exp(-i2\pi c\tilde{\nu}t)\langle \mathbf{M}(t)\mathbf{M}(0)\rangle] \quad (2)$$

In solutions, $\mathbf{M}(t)$ consists of contributions of the dipole moments of the solvent molecule μ_i^{solvent} and the solute molecule μ_k^{solute}. Therefore, in the TCF of $\mathbf{M}(t)$, there are essentially three types of cross terms: a term for the interaction between two different solvent molecules $\langle \mu_i^{\mathrm{solvent}}(t)\mu_j^{\mathrm{solvent}}(0)\rangle$, a term for two different solute molecules $\langle \mu_k^{\mathrm{solute}}(t)\mu_l^{\mathrm{solute}}(0)\rangle$, and a term for the interaction between solvent and solute molecules $\langle \mu_i^{\mathrm{solvent}}(t)\mu_k^{\mathrm{solute}}(0)\rangle$, together with diagonal terms such as $\langle \mu_i^{\mathrm{solvent}}(t)\mu_i^{\mathrm{solvent}}(0)\rangle$ and $\langle \mu_k^{\mathrm{solute}}(t)\mu_k^{\mathrm{solute}}(0)\rangle$.

In order to investigate the dynamics of the solute in the solution, we subtracted the contribution of the solvent to the product spectra $\alpha_{\mathrm{solv}}(\tilde{\nu})n_{\mathrm{solv}}(\tilde{\nu})$ from the solution spectra $\alpha_{\mathrm{soln}}(\tilde{\nu})n_{\mathrm{soln}}(\tilde{\nu})$, and in this way the difference of the product spectra $\Delta[\alpha(\tilde{\nu})n(\tilde{\nu})]$ was obtained

$$\Delta[\alpha(\tilde{\nu})n(\tilde{\nu})] = \alpha_{\mathrm{soln}}(\tilde{\nu})n_{\mathrm{soln}}(\tilde{\nu}) - \alpha_{\mathrm{solv}}(\tilde{\nu})n_{\mathrm{solv}}(\tilde{\nu}) \quad (3)$$

Here, we have assumed that any changes in the density of the solvent due to the presence of solute molecules are negligible.

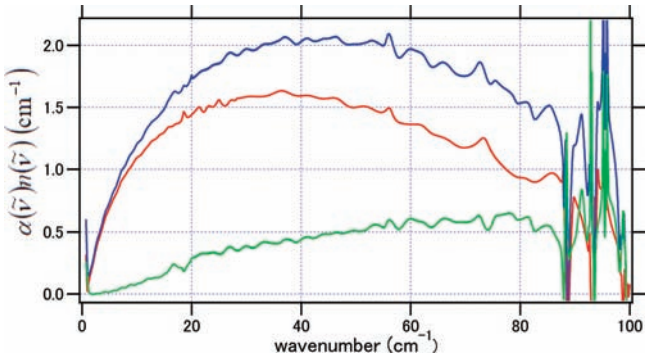

Figure 5. Product spectra $\alpha(\tilde{\nu})n(\tilde{\nu})$ of the solvent cyclohexane (green) and the solution of acetone in cyclohexane (blue) and the difference spectrum between the two spectra (red).

Figure 5 shows the product spectra of the solvent cyclohexane ($\alpha_{solv}(\tilde{\nu})n_{solv}(\tilde{\nu})$, green), the solution of 135 mM acetone in cyclohexane ($\alpha_{soln}(\tilde{\nu})n_{soln}(\tilde{\nu})$, blue), and the difference between the two spectra ($\Delta[\alpha(\tilde{\nu})n(\tilde{\nu})]$, red).

From Figure 2, it is clear that in our experimental conditions, we have observed only the interaction between the solute and solvent, and the interaction between different solute molecules is negligible. Thus, the difference spectrum can be expressed as

$$\Delta[\alpha(\tilde{\nu})n(\tilde{\nu})] \propto \mathrm{Re}[N_{solute}\tilde{\nu}\{1 - \exp(-hc\tilde{\nu}/kT)\}\int_{-\infty}^{\infty} dt \exp(-i2\pi c\tilde{\nu}t)(\langle \mu_k^{solute}(t)\mu_k^{solute}(0)\rangle + 2\sum_i \langle \mu_i^{solvent}(t)\mu_k^{solute}(0)\rangle) \quad (4)$$

where N_{solute} is the number of solute molecules. The second term of eq 4 is multiplied by a factor of 2 since $\sum_i\langle \mu_i^{solvent}(t)\mu_k^{solute}(0)\rangle = \sum_i\langle \mu_k^{solute}(t)\mu_i^{solvent}(0)\rangle$ owing to time reversibility. The first term is related to the orientational dynamics of the solute molecules, and the second term corresponds to the dynamics of the solute in correlation with that of the solvent. In the equation, we can write the two terms separately, as shown in eq 4. The term of $\langle \mu_k^{solute}(t)\mu_k^{solute}(0)\rangle$ represents dynamics of the solute molecule itself such as orientational relaxation of the dipole. On the other hand, the term $\langle \mu_k^{solute}(t)\mu_i^{solvent}(0)\rangle$ represents correlation between the solute and solvent close to the solute. The solute and nearby solvent motions may affect each other. Therefore, it is difficult to separate the two terms spectroscopically. In that sense, we should define the "solute" as a microcluster surrounding the solute molecule. Therefore, we simply express the TCF of the solute by using a single term as follows

$$\langle \mu_{solute}(t)\mu_{solute}(0)\rangle = \langle \mu_k^{solute}(t)\mu_k^{solute}(0)\rangle + 2\sum_i \langle \mu_i^{solvent}(t)\mu_k^{solute}(0)\rangle \quad (5)$$

3.4. Model Time Correlation Functions. The difference $\Delta[\alpha(\tilde{\nu})n(\tilde{\nu})]$ of the product spectra can be analyzed in terms of a different model function for the TCF of $\langle \mu_{solute}(t)\mu_{solute}(0)\rangle$.[22,23] The purpose of this analysis is to find a minimal functional form which can reproduce the experimental results reasonably well. It was reported in our previous studies that in the case of other polar solutes dissolved in nonpolar solvents, a single exponential function for $\langle \mu_{solute}(t)\mu_{solute}(0)\rangle$, i.e.

$$\langle \mu_{solute}(t)\mu_{solute}(0)\rangle = \mu^2 \exp(-t/\tau) \quad (6)$$

is unable to reproduce the experimental data. Figure 6a shows the result for the best fit. This figure clearly shows that an exponential function is incapable of reproducing the experiment in this system. In particular, the intensity of the product spectrum is almost constant in the high-frequency side, which is due to the inappropriate behavior of the TCF near $t = 0$.

Figure 6b shows the simulated curve calculated in accordance to the following functional form

$$\langle \mu_{solute}(t)\mu_{solute}(0)\rangle = \mu^2\left\{\frac{\tau_1}{\tau_1 - \tau_2}\exp(-t/\tau_1) - \frac{\tau_2}{\tau_1 - \tau_2}\exp(-t/\tau_2)\right\} \quad (7)$$

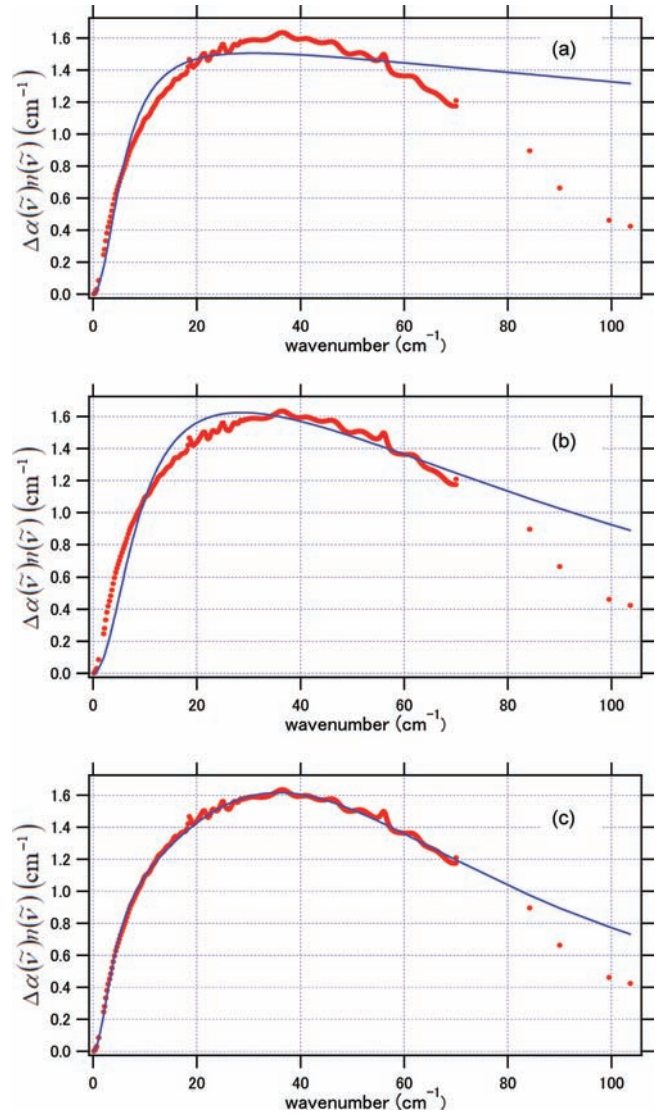

Figure 6. Results of the spectral fitting for the difference product spectra $\Delta\alpha(\tilde{\nu})n(\tilde{\nu})$ with different model functions used as the TCF of the solute dipole moment: (a) eq 6, (b) eq 7, and (c) eq 8. THz-TDS data in the frequency region of 2−70 cm^{-1} are combined with the data reported in ref 15 in the frequency region below 2 cm^{-1} and in the interval of 70−103.6 cm^{-1} and are denoted with red circles. The simulated curves are shown in blue.

In this expression, τ_1 denotes the reorientational relaxation time and τ_2 is the angular velocity correlation time including the inertial effect.[34] It should be noted that this model behaves as $\exp(-t/\tau_1)$ at long times (at low frequency ranges), thus giving rise to diffusive dynamics, and as $(1 - t^2/2\tau_1\tau_2)$ at short times (at high-frequency ranges), provided that $\tau_1 > \tau_2$, where it assumes an asymptotic form which ensures the time reversibility around $t = 0$. However, it is found that eq 7 cannot reproduce the experimentally obtained spectra (Figure 6b).

According to our previous studies,[22,23] if one constructs $\langle\mu_{solute}(t)\mu_{solute}(0)\rangle$ such that it behaves as a biexponential function at long times and as a Gaussian decay at short times, a fairly good agreement between the experiment and the simulation can be obtained

$$\langle\mu_{solute}(t)\mu_{solute}(0)\rangle = \frac{\mu^2}{\tau_2(\tau_1 - \tau_3)a_1 + \tau_1(\tau_2 - \tau_3)a_2} \times \{\tau_1\tau_2(a_1\exp(-t/\tau_1) + a_2\exp(-t/\tau_2)) - (a_1\tau_2 + a_2\tau_1)\tau_3\exp(-t/\tau_3)\} \quad (8)$$

where τ_1 and τ_2 are the time constants of the biexponential relaxation and τ_3 is related to the mean time between collisions. The first part of eq 8 behaves as a biexponential function at long times and as a Gaussian decay $1 - t^2/2\tau_g^2$ at short times. The time constant of the initial Gaussian decay is

$$\tau_g = \sqrt{\frac{\tau_1\tau_2\tau_3\{\tau_2(\tau_1 - \tau_3)a_1 + \tau_1(\tau_2 - \tau_3)a_2\}}{a_1\tau_2^2(\tau_1 - \tau_3) + a_2\tau_1^2(\tau_2 - \tau_3)}} \quad (9)$$

Figure 6c shows the simulated curve corresponding to eq 8. It can be seen that the agreement between the experimental terahertz spectra and the simulated curve shows a satisfactory match, except for the high-frequency region above 70 cm^{-1}. This is one of the main conclusions of this study: a low-frequency spectrum arising from the solute dynamics can be represented fairly well by a biexponential function with an inertial component on a quantitative level. This conclusion is similar to the conclusions of previous studies on solutions of aromatic polar solutes in nonpolar solvents.[22,23]

If we add another high-frequency component, the agreement becomes satisfactory in the whole wavenumber region

$$\langle\mu_{solute}(t)\mu_{solute}(0)\rangle = \frac{A\mu^2}{\tau_2(\tau_1 - \tau_3)a_1 + \tau_1(\tau_2 - \tau_3)a_2}\{\tau_1\tau_2(a_1\exp(-t/\tau_1) + a_2\exp(-t/\tau_2)) - (a_1\tau_2 + a_2\tau_1)\tau_3\exp(-t/\tau_3)\} + (1 - A)\mu^2\exp(-(t/\tau_4)^2) \quad (10)$$

In this equation, the time constant τ_4 corresponds to the additional high-frequency component with a Gaussian function. Figure 7 shows the well-fitted simulated curve, and the values for the parameters obtained by the fitting are given in Table 2. The exponential decay time constants τ_1 and τ_2 are in the picosecond and subpicosecond time scale, respectively. Thus, in order to achieve a better agreement between the experiment and the simulation, the need for an additional high-frequency term is apparent.

Other functional forms which we tested for the TCF include, for example, a single exponential function with an inertial term plus a Gaussian decay, which is expressed as

$$\langle\mu_{solute}(t)\mu_{solute}(0)\rangle = \mu^2\left[a_1\left\{\frac{\tau_1}{\tau_1 - \tau_2}\exp(-t/\tau_1) - \frac{\tau_2}{\tau_1 - \tau_2}\exp(-t/\tau_2)\right\} + a_2\exp(-(t/\tau_3)^2)\right] \quad (11)$$

Although this function provides a moderately good fit to the experimental results, it does not yield satisfactory results. The situation is similar to the simulation performed with eq 8. If we add another high-frequency component, namely

$$\langle\mu_{solute}(t)\mu_{solute}(0)\rangle = \mu^2\left[a_1\left\{\frac{\tau_1}{\tau_1 - \tau_2}\exp(-t/\tau_1) - \frac{\tau_2}{\tau_1 - \tau_2}\exp(-t/\tau_2)\right\} + a_2\exp(-(t/\tau_3)^2) + a_3\exp(-(t/\tau_4)^2)\right] \quad (12)$$

the agreement between the experimental and the simulation becomes fairly good. The optimized time constants τ_3 and τ_4 are 0.43 and 0.19 ps, respectively, while the time constant τ_4 is the same as that in eq 10. The essential point of the results of the spectral simulation is that a picosecond-scale exponential function with an inertial component and an ultrafast decaying component, such as those in eqs 8 and 11, does not provide satisfactory results. In order to obtain a better agreement between the theory and the experiments, it is needed to include a subpicosecond component, such as the $a_2\exp(-t/\tau_2)$ term in eq 10 or the $a_2\exp(-(t/\tau_3)^2)$ term in eq 12.

3.5. Origins of the Spectral Components. We shift the focus of our discussion to the molecular origin of each component in eq 10. In our previous studies, it was reported that the slower exponential component ($\exp(-t/\tau_1)$) has a much greater contribution than the faster component ($\exp(-t/\tau_2)$).[22,23] In this work, we have observed the same trend (Table 2). The

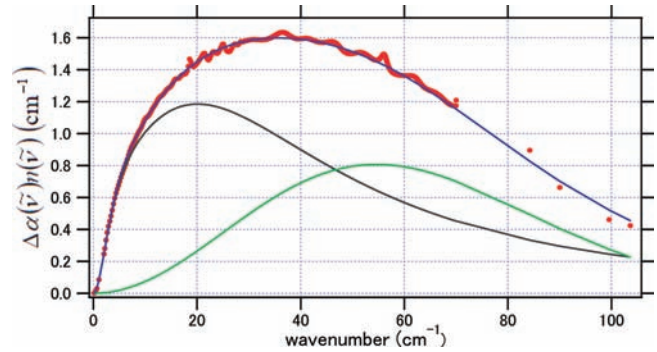

Figure 7. Result of the spectral fitting for the difference product spectra $\Delta\alpha(\tilde{\nu})n(\tilde{\nu})$ with eq 10 for the TCF of the solute dipole moment. THz-TDS data in the frequency region of 2−70 cm^{-1} are combined with the data reported in ref 15 in the frequency region below 2 cm^{-1} and in the interval of 70−103.6 cm^{-1} and are denoted with red circles.

TABLE 2: Parameters Obtained from Equation 10 for a System of Acetone Dissolved in Cyclohexane

A	a_1	τ_1 (ps)	a_2	τ_2 (ps)	τ_3 (ps)	τ_g (ps)	τ_4 (ps)	μ (D)
0.917	0.766	1.480	0.234	0.260	0.130	0.340	0.190	3.43

time constant of the slow component τ_1 is similar to that obtained in the spectral simulation based on eq 1 (1.620 ps). We compare this time constant with the predictions obtained with the SED model. Assuming that the molecular rotation is analogous to the motion of an axiosymmetrical ellipsoidal solute of volume V in a continuous fluid with a shear viscosity η, the SED model yields the following relation for the orientational relaxation

$$\tau_{\mathrm{rot}}^{\ L} = \frac{6 f_L V \eta}{L(L+1) k_{\mathrm{B}} T} \tag{13}$$

In this expression, L is the rank of the considered orientational correlation function ($L = 1$ for the experiment described here), and f_L is a dimensionless rotational friction coefficient dependent on L, which, in a hydrodynamic model, depends on the shape of the rotating molecule as well as on the boundary conditions imposed on the interaction between the molecule and the surrounding fluid.[35−37] The volume of acetone was estimated to be 74 Å^3 from the van der Waals radii of the atoms and the assumed molecular structure with an optimization of the semiempirical molecular orbital method of PM5 performed with MOPAC2002. In this case, the SED model predicts an orientational time of 31 ps for cyclohexane by assuming a spherical molecule and a stick boundary condition ($f_L = 1$), which is much larger than the time constant obtained experimentally. Our previous THz-TDS studies on other polar solutes in nonpolar solvents also report faster time constants compared to the predictions of the SED theory.[22,23] One possible reason for this discrepancy might be the fact that the value of f_L should correspond to a slip boundary condition, which is often pointed out for non-hydrogen bonding solvents. However, the value of f_L should be very small in order to obtain a good agreement between the experimental results and the theoretical prediction, which is physically unrealistic.

Vij and Hufangel pointed out that the anisotropy of the molecular rotation might be one possible origin of the picosecond relaxation.[15] For acetone, the direction of the dipole moment bisects the C−C−C angle. The rotation around the dipolar axis evidently does not produce any changes in the direction of the polarization. There are two more possible degrees of freedom of rotation. The orientational diffusion along an axis perpendicular to the molecular plane of the solute can contribute to the induction of the picosecond component since this motion involves the sweeping of a smaller volume of the solvent, which shows faster orientational diffusion owing to the lower restriction. The slower component of the orientational diffusion, that is, the more restricted orientational diffusion around the axis in the molecular plane, might appear with a much weaker intensity in the spectrum.

In our previous study, we discussed a possible mechanism regarding the molecular origin of the slow component proposed by Smith and Meech.[11] They performed femtosecond OKE measurements with respect to benzene derivatives and mixtures of benzene derivatives with alkane solvents.[11] In these OKE measurements, biexponential relaxation dynamics were observed, where the faster time constants (1−2 ps) of different benzene derivatives in different nonpolar solvents could not be ascribed to orientational diffusion. Smith and Meech suggested that the fast component is more sensitive to local intermolecular interactions between the polar and the polarizable molecules than to the bulk liquid viscosity, and it was proposed that this component arises from structural relaxation occurring on a picosecond time scale in these liquids. In the present THz-TDS study of the system of acetone diluted in cyclohexane, we observed a relaxation time constant of 1.48 ps, which might be also due to local structural decay.

The fast exponential component ($\exp(-t/\tau_2)$) in eq 10 has a relatively small amplitude in comparison to the slow picosecond exponential component, as shown in Table 2. However, this term is necessary for obtaining a reasonably good agreement between the experimental and spectral fits. The exponentially decaying components with subpicosecond time constants have often been observed in ultrafast anisotropy measurements. Knutson and co-workers reported ultrafast components in rotational relaxation measurements of solutions of perylene and tetracene in hexadecane as obtained by femtosecond fluorescence up-conversion.[38] The exponential time constants are in a subpicosecond time scale, which are independent of temperature and viscosity. They suggested the in-plane libration of the molecules within a solvent pocket. Such librational motion should be characterized by a TCF with a Gaussian decay at around $t = 0$. However, if the motion is dumped by collision or friction, the tail of the TCF can be approximated by an exponential function. In this regard, Berg and co-workers reported transient dichroism experiments on anthracene in benzyl alcohol.[39] A fast decay in the subpicosecond region was found and shown to have a viscosity-independent rate. It was assigned to inertial rotation by performing a comparison with computer simulations.[40] The inertial rotation extends out to at least 1 ps, and over a large portion of this range, the inertial rotation is not free-rotor-like but is rather strongly modified by its interaction with the solvent.[41] Currently, we assign the observed subpicosecond component to inertial rotation, which is affected by the surrounding solvent molecules.

As shown in Figure 7, the spectrum of the additional Gaussian component $\exp(-(t/\tau_4)^2)$ in eq 10 (green line) has an amplitude which is comparable with that of the spectrum of the exponential component (black line). In the case where chlorobenzene or nitrobenzene is used as the solute, this Gaussian component has a very weak amplitude in comparison to the components corresponding to the exponential decay.[23] It is not likely that the component is due to some intramolecular mode because there is no strongly IR active mode in this frequency region, which is suggested by quantum chemical calculation. Instead, this component might be due to a librational motion, presumably a tumbling motion of the symmetric top or the rotation around the molecular axis, as suggested by Vij and Hufnagel.[15]

According to our analysis, the ground-state dipole moment of acetone (μ) in the cyclohexane solution is 3.43 D, which is about 15% greater than the dipole moment of acetone in the gas phase. Recently, a theoretical calculation shows that the dipole moment of acetone in an aqueous solution increases by about 60% in comparison to that in the gas phase.[37] An analysis of this result was performed from the viewpoint of mutual electronic polarization of the solute and solvent molecules with regard to the solute−solvent interaction.[37] Although the water molecule is polar and in our case the solvent is purely nonpolar, there is a chance of a slight increase in the dipole moment of the solute due to the interaction between the dipole of the solute and the induced dipole of the solvent or between the dipole of the solute and the quadrapole of the solvent. It should be also noted that if the value of μ of acetone is fixed at its gas phase value in order to simulate the spectra in accordance to eq 11, the parameters listed in Table 2 are not changed significantly.

4. Conclusion

The low-frequency spectra of solutions of acetone in cyclohexane were studied by using THz-TDS at low concentrations ranging between 27 and 135 mM. We obtained the difference spectra of the refractive index $\Delta n(\tilde{\nu})$ and the absorption coefficient $\Delta\alpha(\tilde{\nu})$ between the solutions of acetone in cyclohexane and pure cyclohexane. In the present experimental condition, the spectral intensity follows Beer's law, which indicates the absence of interaction between the solute molecules in the spectrum and the presence of only the solute−solvent interaction. The THz-TDS data were compared with a previously reported dielectric measurement study for this system, and it was found that the inclusion of THz-TDS data improves the spectral quality which clearly suggests the importance of THz-TDS study in the low-frequency region. By combining the previous data and the present results covering the frequency range between 0.2 and 100 cm^{-1}, we performed a spectral simulation in terms of the model function for the total dipole moment of the system. We found that in order to simulate the terahertz spectrum, we need at least a biexponential function with an inertial term and a Gaussian component. The biexponential component has time constants of picosecond and subpicosecond scale, and the Gaussian component is characterized by a subpicosecond time constant. This conclusion is the same as the one drawn from a previous work on systems of aromatic polar solutes in nonpolar solvents, indicating the generality of the claims regarding the interaction between polar solute molecules and nonpolar solvent molecules.

References and Notes

(1) Voth, G. A.; Hochstrasser, R. M. *J. Phys. Chem.* **1996**, *100*, 13034.
(2) Stratt, R. M.; Maroncelli, M. *J. Phys. Chem.* **1996**, *100*, 12981.
(3) Debye, P. *Polar Molecules*; Dover: New York, 1929.
(4) *Rotational Dynamics of Small and Macromolecules*; Dorfmuller, T., Pecora, R., Eds.; Springer-Verlag: Berlin, 1987.
(5) Maroncelli, M. *J. Mol. Liq.* **1993**, *57*, 1.
(6) Jimenez, R.; Fleming, G. R.; Kumar, P. V.; Maroncelli, M. *Nature* **1994**, *369*, 471.
(7) Beard, M. C.; Lotshaw, W. T.; Korter, T. M.; Heilweil, J.; McMorrow, D. *J. Phys. Chem. A* **2004**, *108*, 9348.
(8) Chang, Y. J.; Castner, E. W., Jr. *J. Chem. Phys.* **1993**, *99*, 113.
(9) Loughnane, B. J.; Scodinu, A.; Farrer, R. A.; Fourkas, J. T.; Mohanty, U. *J. Chem. Phys.* **1999**, *111*, 2686.
(10) Giraud, G.; Wynne, K. *J. Chem. Phys.* **2003**, *119*, 11753.
(11) Smith, N. A.; Meech, S. R. *J. Phys. Chem. A* **2000**, *104*, 4223.
(12) Möller, K. D.; Rothschild, W. G. *Far-Infrared Spectroscopy*; Wiley-Interscience: New York, 1971.
(13) Evans, M. *Molecular Dynamics and Theory of Broadband Spectroscopy*; Wiley-Interscience: New York, 1982.
(14) Vij, J. K.; Hufnagel, F. *Chem. Phys. Lett.* **1989**, *155*, 153.
(15) Vij, J. K.; Hufnagel, F. *J. Phys. Chem.* **1991**, *95*, 6142.
(16) *Terahertz Optoelectronics*; Sakai, K., Ed.; Springer: Berlin, 2005.
(17) Schmuttenmaer, C. A. *Chem. Rev.* **2004**, *104*, 1759.
(18) Flanders, B. N.; Cheville, R. A.; Grischkowsky, D.; Scherer, N. F. *J. Phys. Chem.* **1996**, *100*, 11824.
(19) Schrödle, S.; Fischer, B.; Helm, H.; Buchner, R. *J. Phys. Chem. A* **2007**, *111*, 2043.
(20) Yamamoto, K.; Tani, M.; Hangyo, M. *J. Phys. Chem. B* **2007**, *111*, 48.
(21) Oka, A.; Tominaga, K. *J. Non-Cryst. Solids* **2006**, *352*, 4606.
(22) Dutta, P.; Tominaga, K. *J. Mol. Liq.* **2009**, *147*, 45.
(23) Dutta, P.; Tominaga, K. *Mol. Phys.*, in press.
(24) Nagai, M.; Yada, H.; Arikawa, T.; Tanaka, K. *Int. J. IRMMW* **2006**, *27*, 505.
(25) Arikawa, T.; Nagai, M.; Tanaka, K. *Chem. Phys. Lett.* **2008**, *457*, 12.
(26) Heugen, U.; Schwaab, G.; Bründermann, E.; Heyden, M.; Yu, X.; Leitner, D. M.; Havenith, M. *Proc. Natl. Acad. Sci. U.S.A.* **2006**, *103*, 12301.
(27) Heyden, M.; Bründermann, E.; Heugen, U.; Niehues, G.; Leitner, D. M.; Havenith, M. *J. Am. Chem. Soc.* **2008**, *130*, 5773.
(28) Leroy, Y.; Constant, E.; Abbar, C.; Desplanques, P. *Adv. Mol. Relax. Processes* **1967/68**, *1*, 273.
(29) Arnold, K. E.; Yarwood, J.; Price, A. H. *Mol. Phys.* **1983**, *48*, 451.
(30) Klages, G. *Z. Naturforsch.* **1988**, *43a*, 1.
(31) Yamamato, K.; Tominaga, K.; Sasakawa, H.; Tamura, A.; Murakami, H.; Ohtake, H.; Sarukura, N. *Bull. Chem. Soc. Jpn.* **2002**, *75*, 1083.
(32) Yamamoto, K.; Kabir, M. H.; Hayashi, M.; Tominaga, K. *Phys. Chem. Chem. Phys.* **2005**, *7*, 1945.
(33) McQuarrie, D. A. *Statistical Mechanics*; University Science Books: Sausalito, CA, 2000.
(34) Birnbaum, G.; Cohen, E. R. *J. Chem. Phys.* **1970**, *53*, 2885.
(35) Horng, M.-L.; Gardecki, J. A.; Maroncelli, M. *J. Phys. Chem.* **1997**, *101*, 1030.
(36) Perrin, F. *J. Phys. Radium* **1934**, *33*, 497.
(37) Dote, J. L.; Kivelson, D.; Schwartz, R. N. *J. Phys. Chem.* **1981**, *85*, 2169.
(38) Xu, J.; Shen, X.; Knutson, J. *J. Phys. Chem. A* **2003**, *107*, 8383.
(39) Zhang, Y.; Sluch, M. I.; Somoza, M. M.; Berg, M. A. *J. Chem. Phys.* **2001**, *115*, 4212.
(40) Jas, G. S.; Wang, Y.; Pauls, S. W.; Johnson, C. K.; Kuczera, K. *J. Chem. Phys.* **1997**, *107*, 8800.
(41) Georg, H. C.; Coutinho, K.; Canuto, S. *Chem. Phys. Lett.* **2006**, *429*, 119.

JP900488C